Optically mediated coherent population trapping in asymmetric semiconductor quantum wells

J. F. Dynes,* M. D. Frogley, J. Rodger, and C. C. Phillips
Experimental Solid State Group, Department of Physics, Imperial College, Prince Consort Road, London SW7 2BZ, United Kingdom
(Received 25 April 2005; published 9 August 2005)

A quantum well (QW), with only three transitions, which are all dipole allowed because of the QW asymmetry, is investigated when driven coherently by two infrared optical fields. One field couples the $|1\rangle - |2\rangle$ and $|2\rangle - |3\rangle$ transitions simultaneously, while a second field couples the $|1\rangle - |3\rangle$ transition. The absorption linear response is computed allowing the illustration of some features due to quantum coherence. Without the second field, the absorption of a weak probe is that of a strongly saturated system. As the coupling strength of the second field is increased the absorption strength of a weak probe increases, by over an order of magnitude factor in absorption strength compared to the case in the absence of the second field. The results are shown to be due to an optically mediated, coherent population trapping effect.

DOI: 10.1103/PhysRevB.72.085323 PACS number(s): 78.67.De, 42.50.Hz, 03.67.Lx

I. INTRODUCTION

Intersubband transitions (ISBTs) in the conduction band of semiconductor quantum wells (QW's) have recently attracted attention for studying optical nonlinear and coherent effects. Due to strong electron-electron interactions, the two-dimensional electron gas behaves effectively as a single oscillator[1–3] and atomiclike ISBT absorption responses result. The large dipole matrix elements give rise to sizeable Rabi frequencies, which corresponds to fast Rabi oscillations in the time domain. These fast oscillations allow coherent processes to occur on time scales shorter than the ISBT dipole dephasing time. The ISBT energies and electron wavefunction symmetries can be engineered, with a flexibility unknown in atomic systems, to suit particular requirements. These developments in semiconductor growth technology have led to the observation of optical nonlinear and coherent effects; for example, intersubband Rabi splitting,[4] electromagnetically induced transparency (EIT),[5] and EIT in interband excitons.[6]

A symmetric quantum well with three energy levels forms the well-known "cascade" configuration, where the first to second and second to third ISBTs are dipole allowed but the first to third ISBT is dipole forbidden on the basis of parity considerations [Fig. 1(a)]. Driving the two dipole allowed ISBTs with two optical fields of arbitrary strengths has been studied previously in the context of examining the small signal absorption response.[7] This was a demonstration of gain and absorption in such a driven system. In an asymmetric quantum well however, all possible transitions are dipole allowed (to varying degrees). This permits, for example, the formation of a close relative to the so-called Λ system: with one optical field coupling the first to third ISBT and a second coupling the second to third ISBT [Fig. 1(b)].[8,9]

The Λ system in atomic physics is a well-studied configuration and normally employed for the study of coherent population trapping (CPT), another well-known effect which is closely related to EIT. CPT involves the creation of a so-called "dark state" by preparing the atomic system with strong resonant, optical fields such that the population decay from an upper level into the dark state becomes trapped and consequently there is negligible absorption from this state.[10] Two strong optical fields are tuned resonantly to the two dipole allowed transitions of the Λ system causing the bare states to become dressed into quantum superpositions. The time scale for CPT to occur is several radiative lifetimes; EIT, which happens on a time scale of the order of the reciprocal of the Rabi frequency of the transition-optical field coupling, is much faster.

In this paper we examine the effect of driving all three possible transitions, each possessing significant nonzero dipoles, of a three-level QW system; all dipoles are coupled by the interaction of strong optical fields. Actually, this system can be realized experimentally with only one laser frequency such as that derived from a carbon dioxide laser. The fundamental carbon dioxide laser frequency couples both the $|1\rangle - |2\rangle$ and the $|2\rangle - |3\rangle$ transitions simultaneously and the $|1\rangle - |3\rangle$ transition is coupled by the second harmonic frequency of the carbon dioxide laser, achieved by frequency doubling in an appropriate nonlinear crystal. The small signal absorption spectrum of a weak probe propagating through such a driven system is computed in the steady state. By steady state we mean that the strong optical fields are applied to the system for long enough such that all transients have died away before calculating the small signal absorption. To our knowledge this is the first report of small signal absorption and gain in such a driven system in the steady state. It is emphasized from the outset that our treatment is general in that the three dipole couplings can have different optical fre-

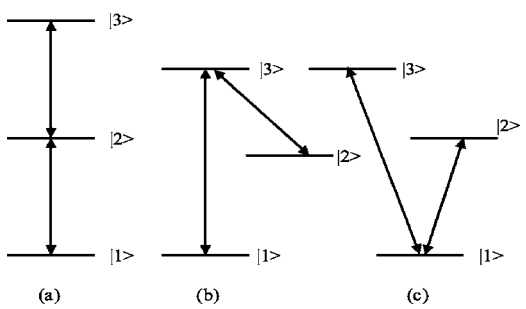

FIG. 1. Three level energy schemes for interaction with one or more resonant coupling fields (derived from Ref. 10). (a) Cascade (ladder) (b) lambda, and (c) V schemes.

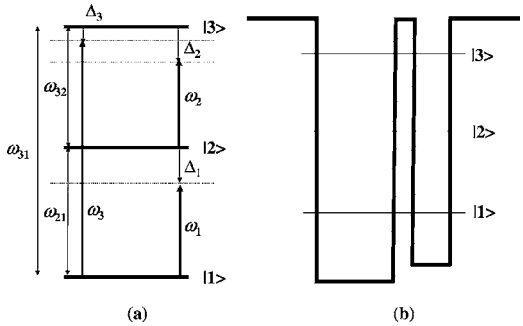

FIG. 2. Schematic of the energy level arrangement for the asymmetric quantum wells considered in this paper. Subband levels are labeled in ascending energy: $|1\rangle$, $|2\rangle$, and $|3\rangle$. There are three possible optical transitions (frequencies): $|1\rangle-|2\rangle$ (ω_{21}), $|2\rangle-|3\rangle$ (ω_{32}), and $|1\rangle-|3\rangle$ (ω_{31}). Three coupling fields with optical frequencies ω_1, ω_2, and ω_3 couple separately to the transitions $|1\rangle-|2\rangle$, $|2\rangle-|3\rangle$, and $|1\rangle-|3\rangle$, respectively. The coupling field detunings from the transition frequencies are defined as $\Delta_1=\omega_{21}-\omega_1$, $\Delta_2=\omega_{32}-\omega_2$, and $\Delta_3=\omega_{31}-\omega_3$. (b) Schematic of the asymmetric conduction band barrier arrangement to create an asymmetric quantum well in which all transitions are dipole allowed.

quencies (with corresponding detunings from the QW ISBT's). Physically we explain the effect in terms of dressed state pictures and CPT.

The paper is organized as follows: Section II develops the theoretical formalism for a conduction band three-level QW coupled by three independent, strong optical fields. The section also outlines very briefly the method for computing the ISBT small signal absorption spectrum in steady state conditions. In Sec. III the results for resonantly and off resonantly driven three-level QWs, using the fundamental and second harmonic of a single strong optical field are presented. The spectra are interpreted using dressed state pictures. A discussion of the results and conclusions is made in Sec. IV.

II. THEORY

We consider a n doped three-level asymmetric quantum well with three dipole-allowed conduction band ISBT's as depicted in Fig. 2. Three infrared fields with optical frequencies ω_1, ω_2, and ω_3 are assumed to be coupled individually to the ISBTs frequencies ω_{21}, ω_{32}, and ω_{31}, respectively. In the interaction representation, and under the rotating wave approximation, the interaction Hamiltonian H_{int} is given by

$$\mathcal{H}_{int}=\hbar\Omega_1(a_2^\dagger a_1 e^{i\Delta_1 t}+a_1^\dagger a_2 e^{-i\Delta_1 t})+\hbar\Omega_2(a_3^\dagger a_2 e^{i\Delta_2 t}+a_2^\dagger a_3 e^{-i\Delta_2 t})+\hbar\Omega_3(a_3^\dagger a_1 e^{i\Delta_3 t}+a_1^\dagger a_3 e^{-i\Delta_3 t}), \quad (1)$$

where Ω_i are the corresponding Rabi frequencies of the coupling fields, Δ_i are the ISBT transition detunings given by $\Delta_1=\omega_{21}-\omega_1$, $\Delta_2=\omega_{32}-\omega_2$, and $\Delta_3=\omega_{31}-\omega_1$, and $a_i^\dagger$ and a_i are the electron creation and annihilation operators, respectively, for level i.

The time evolution of Eq. (1), expressed using the density operator ρ, is governed by the Liouville equation which is, in the interaction representation

$$\frac{d\rho}{dt}=-\frac{i}{\hbar}[\mathcal{H}_{int},\rho]+\Gamma, \quad (2)$$

where Γ represents the irreversible decay processes which we treat phenomenologically; the details and justification of such an approach will be made shortly. The explicit form of Eq. (2) becomes

$$\frac{d\rho_{12}}{dt}=-i\Omega_1 e^{-i\Delta_1 t}(\rho_{22}-\rho_{11})+i\Omega_2 e^{i\Delta_2 t}\rho_{13}-i\Omega_3 e^{-i\Delta_3 t}\rho_{32}-\gamma_{12}\rho_{12}, \quad (3a)$$

$$\frac{d\rho_{23}}{dt}=-i\Omega_2 e^{-i\Delta_2 t}(\rho_{33}-\rho_{22})-i\Omega_1 e^{i\Delta_1 t}\rho_{13}+i\Omega_3 e^{-i\Delta_3 t}\rho_{21}-\gamma_{23}\rho_{23}, \quad (3b)$$

$$\frac{d\rho_{13}}{dt}=-i\Omega_3 e^{-i\Delta_3 t}(\rho_{33}-\rho_{11})-i\Omega_1 e^{-i\Delta_1 t}\rho_{23}+i\Omega_2 e^{-i\Delta_2 t}\rho_{12}-\gamma_{13}\rho_{13}, \quad (3c)$$

$$\frac{d\rho_{22}}{dt}=-i\Omega_1 e^{i\Delta_1 t}\rho_{12}+i\Omega_1 e^{-i\Delta_1 t}\rho_{21}-i\Omega_2 e^{-i\Delta_2 t}\rho_{32}+i\Omega_2 e^{i\Delta_2 t}\rho_{23}-\gamma_2\rho_{22}+\gamma_3\rho_{33}, \quad (3d)$$

$$\frac{d\rho_{33}}{dt}=-i\Omega_3 e^{i\Delta_3 t}\rho_{13}+i\Omega_3 e^{-i\Delta_3 t}\rho_{31}-i\Omega_2 e^{-i\Delta_2 t}\rho_{32}-i\Omega_2 e^{i\Delta_2 t}\rho_{23}-(\gamma_1+\gamma_3)\rho_{33}, \quad (3e)$$

together with $\rho_{ij}=\rho_{ji}^\star$. Actually, because of the additional population conservation condition $\rho_{11}+\rho_{22}+\rho_{33}=1$, Eq. (3) generates a set of eight linearly independent equations. The population scattering rates γ_i are due primarily to longitudinal optical (LO) phonon emission events at low temperature.[11] The total dephasing rates[12] $\gamma_{ij}(i\neq j)$ are given by $\gamma_{12}=(\gamma_2+\gamma_{12}^{dph})$, $\gamma_{23}=(\gamma_1+\gamma_2+\gamma_3+\gamma_{23}^{dph})$, and $\gamma_{13}=(\gamma_1+\gamma_3+\gamma_{13}^{dph})$, where the pure dipole dephasing rates γ_{ij}^{dph} are assumed to be due to a combination of quasielastic interface roughness scattering or acoustic phonon scattering.[4] A comprehensive treatment of the decay rates would involve incorporation of the decay mechanisms into the Hamiltonian (1). However, at the risk of slightly losing generality, we adopt the phenomenological approach of treating the decay mechanisms. The immediate payoff of is that the underlying complexity of coupling all three transitions is not further obscured by complicating the Hamiltonian further. In the past this phenomenological approach has proven well suited to modeling experimental results.[5]

Equations (3) can be cast more neatly as a vector equation

$$\frac{d\Psi(t)}{dt}=L(t)\Psi(t), \quad (4)$$

where Ψ is a nine element column vector with elements defined as

$$\Psi(t) = (\Psi_1, \Psi_2, \ldots, \Psi_9) = (\rho_{12}, \rho_{13}, \rho_{23}, \rho_{21}\rho_{31}, \rho_{32}, \rho_{22}, \rho_{33}, \rho_{11}), \tag{5}$$

and L is the nine-by-nine matrix

$$L = \begin{pmatrix}
-\gamma_{12} & i\Omega_2 e^{i\Delta_2 t} & 0 & 0 & 0 & i\Omega_3 e^{i\Delta_3 t} & i\Omega_1 e^{i\Delta_1 t} & 0 & i\Omega_1 e^{-i\Delta_1 t} \\
i\Omega_2 e^{-i\Delta_2 t} & -\gamma_{13} & i\Omega_1 e^{-i\Delta_1 t} & 0 & 0 & 0 & 0 & -i\Omega_3 e^{-i\Delta_3 t} & i\Omega_3 e^{-i\Delta_3 t} \\
0 & i\Omega_1 e^{i\Delta_1 t} & -\gamma_{23} & i\Omega_3 e^{-i\Delta_3 t} & 0 & 0 & i\Omega_2 e^{-i\Delta_2 t} & -i\Omega_2 e^{i\Delta_2 t} & 0 \\
0 & 0 & i\Omega_3 e^{i\Delta_3 t} & -\gamma_{12} & -i\Omega_2 e^{-i\Delta_2 t} & 0 & i\Omega_1 e^{i\Delta_1 t} & 0 & i\Omega_1 e^{-i\Delta_1 t} \\
0 & 0 & 0 & -i\Omega_2 e^{i\Delta_2 t} & -\gamma_{13} & i\Omega_1 e^{i\Delta_1 t} & 0 & i\Omega_3 e^{i\Delta_3 t} & i\Omega_3 e^{-i\Delta_3 t} \\
-i\Omega_3 e^{-i\Delta_3 t} & 0 & 0 & 0 & i\Omega_1 e^{-i\Delta_1 t} & -\gamma_{23} - i\Omega_2 e^{i\Delta_2 t} & i\Omega_2 e^{i\Delta_2 t} & 0 & \\
-i\Omega_1 e^{i\Delta_1 t} & 0 & -i\Omega_2 e^{i\Delta_2 t} & i\Omega_1 e^{-i\Delta_1 t} & 0 & -i\Omega_2 e^{-i\Delta_2 t} & -\gamma_2 & \gamma_3 & 0 \\
0 & -i\Omega_3 e^{i\Delta_3 t} & -i\Omega_2 e^{i\Delta_2 t} & 0 & i\Omega_3 e^{-i\Delta_3 t} & i\Omega_2 e^{-i\Delta_2 t} & 0 & -(\gamma_1 + \gamma_3) & 0 \\
i\Omega_1 e^{i\Delta_1 t} & i\Omega_3 e^{i\Delta_3 t} & 0 & -i\Omega_1 e^{-i\Delta_1 t} & -i\Omega_3 e^{-i\Delta_3 t} & 0 & \gamma_2 & \gamma_1 & 0
\end{pmatrix}. \tag{6}$$

Note the explicit time dependence contained in the matrix L. To solve Eq. (4), previous approaches have eliminated the time dependence completely,[13] with the purpose of extracting only the steady state solution. We retain the explicit time dependence so as to examine possible solutions to Eq. (4) that do not possess a steady state solution. For illustration purposes we now apply this to a three-level, asymmetric QW with equal ISBT energy separations $|1\rangle - |2\rangle$ and $|2\rangle - |3\rangle = 125$ meV so $|1\rangle - |3\rangle = 250$ meV and with all the ISBT's are all dipole allowed. The choice of population decay rates and dephasing rates are based on the results of Refs. 5 and 14. We set $\gamma_i = 1$ meV ($i = 1$, 2, and 3) and $\gamma_{12} = \gamma_{23} = \gamma_{13} = 5$ meV appropriate for existing QW low temperature experiments. The time evolution of this system is governed by Eq. (4) with the initial density matrix vector, $\Psi(0) = (0,0,0,0,0,0,0,0,1)$. Three resonant optical fields, $\hbar\omega_1 = \hbar\omega_2 = 125$ meV and $\hbar\omega_3 = 250$ meV (Rabi frequencies: $r_1 = r_2 = r_3 = 5$ meV) to the transitions $|1\rangle - |2\rangle$, $|2\rangle - |3\rangle$, and $|1\rangle - |3\rangle$, respectively, are then applied at time $t = 0$. Using standard numerical techniques,[15] Eq. (4) are integrated to yield the time responses of the diagonal density matrix elements, i.e., the populations for all three levels $|1\rangle$, $|2\rangle$, and $|3\rangle$. As can be seen from the results plotted in Fig. 3(a), when the strong, resonant optical fields are applied at $t = 0$, the populations experience rapid Rabi oscillations of a time period 200–300 fs, but reach steady state conditions within a couple of Rabi periods. In fact all the density matrix elements now reach steady state values after 4–5 ps (the long time limit).

Now consider the case when one or more of the strong optical fields are detuned from their respective transition(s). For example, consider the detunings: $\Delta_1 = \Delta_2 = 0$ and $\Delta_3 = 10$ meV. The equations of motion are again numerically integrated, but it is found under these detunings, the systems' density matrix elements never achieve steady state conditions Fig. 3(b). This poses a problem for the calculation of the small signal spectra for such a system by using standard linear response theory, which is employed in the next section, as the systems' density matrix elements are no longer stationary. We will therefore restrict our analysis to the cases where the detunings obey the relationship $\Delta_3 - \Delta_2 - \Delta_1 = 0$, as these always yield steady state results for the density matrix elements. It is easy to achieve this criterion through an experimental arrangement based on a frequency doubling scheme as shown in the following section.

We adopt the procedure of Manka *et al.*[16] to calculate the linear absorption response. The absorption coefficient of a weak probe with optical frequency ω is given by[17]

$$\alpha(\omega) = \text{constant} \times \mathcal{F}\langle[\mu^+, (\tau)\mu^-(0)]\rangle, \tag{7}$$

where $\mathcal{F}$ denotes the Fourier transform operation, $\mu = \mu^+ + \mu^-$ is the dipole operator (at times, $t = 0$ and $t = \tau$), and is decomposed into positive and negative parts for the three-level quantum well system as

$$\mu^+ = \mu_{12} a_1^\dagger a_2 + \mu_{23} a_2^\dagger a_3 + \mu_{13} a_1^\dagger a_3 \tag{8}$$

and μ^- is given by the complex conjugate of μ^+.

We use the quantum regression theorem[18] to derive expressions for Eq. (7) to evaluate the two-time expectation values in Eq. (7). The Liouville equation is integrated twice: once to yield the steady state density matrix elements and secondly to yield the two-time expectation values.[16]

III. SMALL SIGNAL ABSORPTION IN A RESONANTLY DRIVEN SEMICONDUCTOR QUANTUM WELL

To keep the analysis appropriate to an experimental realization, for definiteness, we consider the case of the frequencies of driving fields ω_1 and ω_2 to be equal: $\omega_1 = \omega_2$. As mentioned in the Introduction, these fields could be conveniently provided by a single CO_2 laser. The third field, $\omega_3 = 2\omega_1$ could be supplied by the second harmonic of the CO_2 laser through frequency upconversion in a nonlinear crystal. It is not necessary to be concerned with the phase relationship of the laser fundamental frequency and second harmonic frequency as they will be necessarily phase locked. Note that the use of this scheme implies the restriction on the

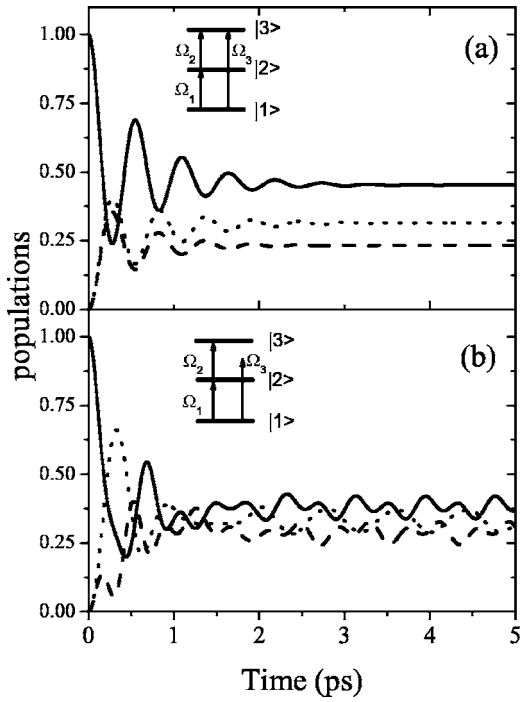

FIG. 3. Time evolution of the QW electron populations for all three levels $|1\rangle$ (solid line), $|2\rangle$ (dotted line), and $|3\rangle$ (dashed line) in the presence of three driving optical fields, each possessing Rabi frequencies $\Omega_1=\Omega_2=\Omega_3=5$ meV from $t=0$ (when the fields were switched on). (a) Under resonant driving conditions, $\Delta_1=\Delta_2=\Delta_3=0$ and (b) under a detuned driving configuration, $\Delta_1=\Delta_2=0$ and $\Delta_3=10$ meV.

optical field detunings, namely, $\Delta_3-\Delta_2-\Delta_1=0$. This condition automatically satisfies the requirement that the system's density matrix elements attain steady state values in the long time limit, as required by linear response theory.

To obtain ISBT's with these energies, we have numerically solved the one-dimensional Schrödinger equation self-consistently and found that it is possible to create a three-level QW with the equal transition energies (dipole matrix elements) $\hbar\omega_{21}=\hbar\omega_{32}$ $(\mu_{21}=\mu_{32})$ and of course $\hbar\omega_{31}=2\hbar\omega_{21}=2\hbar\omega_{32}$. We choose $\hbar\omega_{21}=125$ meV, $\hbar\omega_{32}=125$ meV, and $\hbar\omega_{31}=250$ meV with equal dipole matrix elements $\mu_{21}=\mu_{32}$ of the order of 1 nm (and μ_{31} is less than 1 nm). The choice of population decay rates and dephasing rates are (as in Sec. I) based on the experimental results for similar QWs of references:[5,14] $\gamma_i=1$ meV $(i=1,2,3)$ and $\gamma_{12}=\gamma_{23}=\gamma_{13}=5$ meV. The effect of driving all three transitions simultaneously with resonant, strong optical fields $(\Delta_3=\Delta_2=\Delta_1=0)$ is shown in Fig. 4. Figure 4(a) shows the total linear absorption response $\alpha(\omega)$ with the Rabi frequencies $\Omega_1=\Omega_2=\Omega_3=0$. Using the single laser optical field from the fundamental of the CO_2 laser corresponding Rabi frequencies of $\Omega_1=\Omega_2=5$ meV can be obtained (owing to the equal dipole matrix elements $\mu_{21}=\mu_{32}$) resulting in a Mollow-like spectrum[17] with five identifiable absorption spectral peaks and four gain features [dotted line, Fig. 4(b)]. The system is strongly saturated, meaning the population is almost evenly distributed through all three levels. A qualitatively different spectrum results when the second harmonic

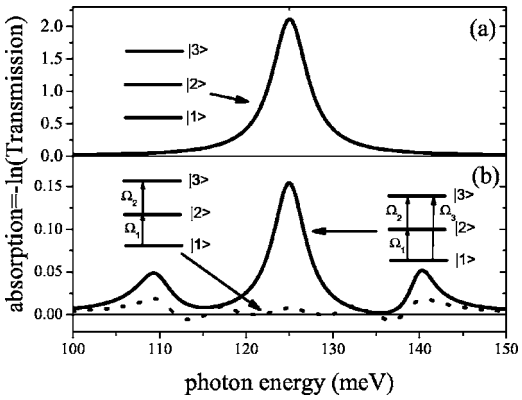

FIG. 4. Linear absorption response of an asymmetric quantum well (transition frequencies: $\omega_{21}=\omega_{32}=125$ mev and $\omega_{31}=250$ meV) in the frequency range of both the $|1\rangle-|2\rangle$ and $|2\rangle-|3\rangle$ transitions under the resonant coupling field configuration of $\omega_1=\omega_2=125$ meV and $\omega_3=250$ meV (the detunings are all zero). (a) $\Omega_1=\Omega_2=\Omega_3=0$; Lorentzian linear absorption response of the transitions $|1\rangle-|2\rangle$ and $|2\rangle-|3\rangle$. (b) Dotted line: $\Omega_1=\Omega_2=5$ meV and $\Omega_3=0$. Solid line $\Omega_1=\Omega_2=\Omega_3=5$ meV. In all cases $\gamma_i=1$ meV $(i=1,2,3)$ and $\gamma_{12}=\gamma_{23}=\gamma_{13}=5$ meV.

of the laser optical field is also applied such that all three Rabi frequencies are the same $[\Omega_1=\Omega_2=\Omega_3=5$ meV, solid line, Fig. 4(b)]. The central frequency absorption coefficient at probe frequency $\omega=125$ meV increases by almost a factor of 20 and the number of spectral absorption peaks reduces from five to three.

Further increasing the intensity of the second harmonic beam, i.e., increasing the Rabi frequency Ω_3, results in the system becoming saturated again and the concomitant revival of the five spectral absorption peaks. The evolution of the absorption spectrum as Ω_3 is increased from 0–10 meV is shown by the three-dimensional (3D) plot, Fig. 5. The critical point to note is that since the QW system is asymmetric, a different effect has occurred. The absorption coef-

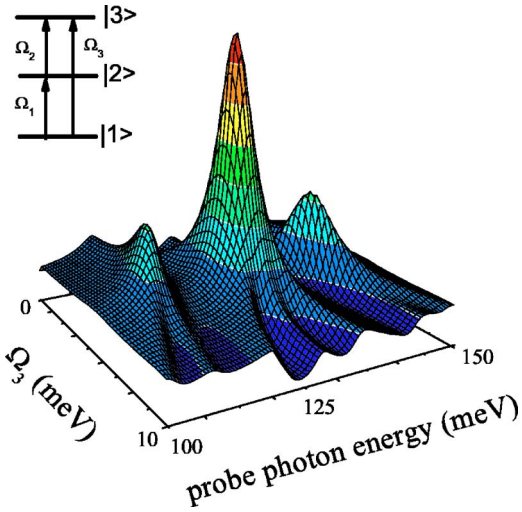

FIG. 5. (Color online) Three-dimensional plot [for the parameters in Fig. 4(b) solid line] depicting the evolution of the linear absorption spectrum of both the $|1\rangle-|2\rangle$ and $|2\rangle-|3\rangle$ transitions as a function of Ω_3 (Ω_1 and Ω_2 are held fixed at 5 meV).

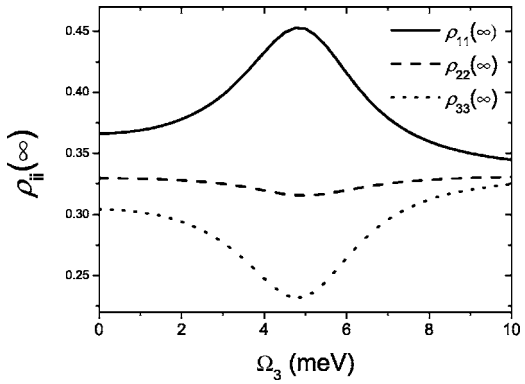

FIG. 6. Steady state populations $\rho_{ii}(\infty)$ of levels $|1\rangle$, $|2\rangle$, and $|3\rangle$ ($\rho_{11}(\infty)$, $\rho_{22}(\infty)$, and $\rho_{33}(\infty)$, respectively, as a function of coupling field Rabi frequency Ω_3. The parameters for the asymmetric quantum well transition frequencies and coupling field configuration is given in the caption of Fig. 2.

ficient at $\omega_{12}=125$ meV has been increased by over an order of magnitude by the *application* of an additional strong field.

To understand the physical mechanism behind these results, it helps to examine the steady state electron populations (Fig. 6), as a function of Ω_3. As Ω_3 is increased, the population in level $|1\rangle$, $\rho_{11}(\infty)$ increases peaking at a value around $\Omega_3=5$ meV, while the population of level $|3\rangle$, $\rho_{33}(\infty)$, empties to a minimum value. Some of the population from level $|3\rangle$ has been confined in level $|1\rangle$ by the coupling field ω_3. This results in the enhanced absorption for the transitions ω_{21}. For the transition ω_{32}, the absorption is enhanced as well, since there is a smaller population in level $|3\rangle$ now and stimulated emission on this transition is reduced. This absorption enhancement occurs despite the fact that the coupling strength of the $|1\rangle-|3\rangle$ transition has been increased due to the presence of coupling field ω_3; one would perhaps intuitively expect that with the addition of this extra field, the QW becomes further saturated. This however, is not the case. The result can be explained in terms of coherent population trapping (CPT). CPT normally occurs when the two-photon (or Raman) $|1\rangle-|3\rangle$ transition is mediated by the near resonant one-photon coupling fields ω_1 and ω_2.[10] In our case, the

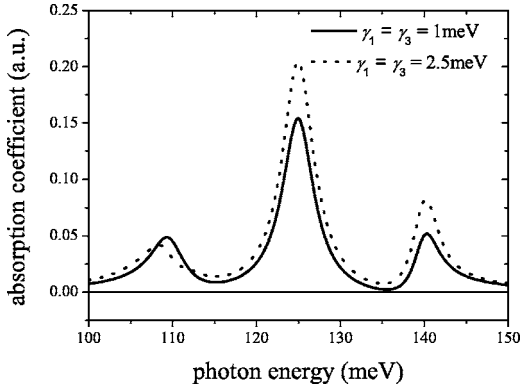

FIG. 7. Comparison of the linear absorption response for the driven system of Fig. 4 for two different regimes of the level $|3\rangle$ population decay rate. Solid line: $\gamma_1=\gamma_3=1$ meV. Dotted line: $\gamma_1=\gamma_3=2.5$ meV.

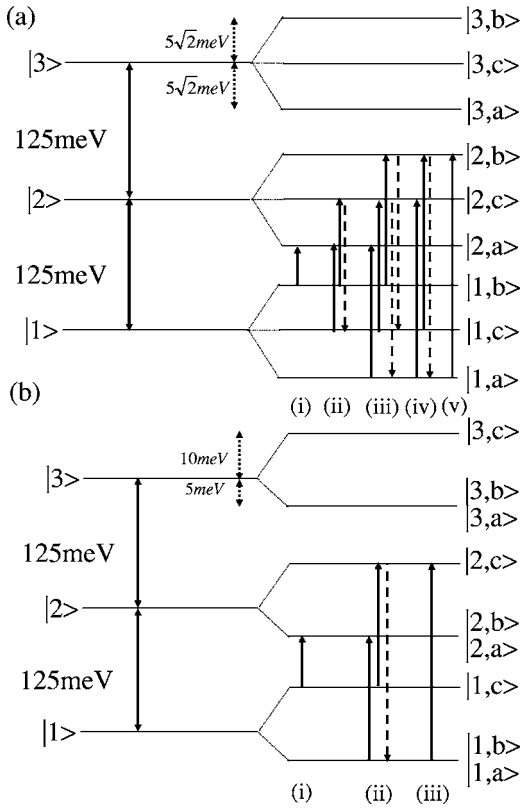

FIG. 8. Schematics of the dressed state pictures for a triply driven three level QW by three strong driving fields. (a) $\Omega_1=\Omega_2=5$ meV and $\Omega_3=0$. We obtain symmetric splitting of the three original eigenstates, $|1\rangle$, $|2\rangle$, and $|3\rangle$. Each level has now developed into a triplet of dressed energy eigenstates. The energy separation of these triplet states is equal: $|i,a\rangle\rightarrow|i,c\rangle=5\sqrt{2}$ meV and $|i,c\rangle\rightarrow|i,b\rangle=5\sqrt{2}$ meV, where i is the original eigenstate label, 1, 2, or 3. There are five spectral contributions to the absorption spectrum, denoted by the absorption routes (solid arrows) and gain routes (dotted arrows) (i)–(v) (for $i=1,2$). (b) $\Omega_1=\Omega_2=\Omega_3=5$ meV. Now the triplet reduces to an asymmetric doublet (as the two dressed states are degenerate). The energy separations of the states are now: $|i,a\rangle\rightarrow|i,b\rangle=0$ and $|i,a\rangle\rightarrow|i,c\rangle$ and $|i,b\rangle\rightarrow|i,c\rangle=15$ meV. There are three spectral contributions to the absorption spectrum, denoted by the absorption routes (solid arrows) and gain routes (dotted arrows) (i)–(iii) (for $i=1,2$). There is an identical set of absorption/gain contributions for $i=2,3$.

two-photon coupling is replaced by the (one-photon) coupling field ω_3. When the Rabi frequency Ω_3 approaches the values of Ω_1 and Ω_2, population is transferred to level $|1\rangle$ from level $|3\rangle$ through the CPT effect. State $|1\rangle$ has become a dark state compared to level $|3\rangle$ but not compared to level $|2\rangle$: Absorption occurs strongly for $|1\rangle-|2\rangle$ and also for $|2\rangle-|3\rangle$. Moreover, the total population decay rate of level $|3\rangle$ governs the effectiveness of the CPT effect: If the population decay rate of level $|3\rangle$ into level $|1\rangle$ is increased in the model, more population is transferred to level $|1\rangle$ and the linear absorption response further increases (dotted line, Fig. 7). The population rate is dependent on the electron-LO phonon scattering times and is governed by[4]

$$(z_{i,i-1}/q_{\parallel})^2, \tag{9}$$

where z_{ij} is the matrix element between the levels i and j involved in the scattering event, and $q_{\parallel}$ is the corresponding in-plane LO-phonon wave vector emitted when an electron (effective mass $m^{\star}$) scatters from the $|i\rangle \rightarrow |j\rangle$ subband: $q_{\parallel} = [2m^{\star}(\hbar\omega_{ij} - \hbar\omega_{LO})\hbar^2]^{1/2}$. This implies a γ_3 population decay rate which decays monotonically as ω_{31} is increased by changing the QW design. For QWs with a small ω_{31} (and hence a large γ_3), the coupling to the second harmonic field ω_3, is enhanced, while coupling to both the ω_1 and ω_2 fields is inhibited. This is analogous to the predictions for CPT in a QW Λ scheme.[19]

To understand the origin of the spectral features in Fig. 4(b) we can adopt a dressed state approach. Without the presence of the second harmonic beam, i.e., when $\Omega_1 = \Omega_2 = 5$ meV and $\Omega_3 = 0$ meV, the energy eigenvectors (or dressed states) obtained by diagonalizing Eq. (1), are a triplet of states $|a\rangle$, $|b\rangle$, and $|c\rangle$,

$$|a\rangle = \frac{1}{2}(|1\rangle - \sqrt{2}|2\rangle + |3\rangle), \quad |b\rangle = \frac{1}{2}(|1\rangle + \sqrt{2}|2\rangle + |3\rangle),$$

$$|c\rangle = \frac{1}{\sqrt{2}}(|3\rangle - |1\rangle), \tag{10}$$

which are each separated from each other by an equal energy of $5\sqrt{2}$ meV, Fig. 8(a). Between a pair of these triplets, separated by the coupling field frequency of 125 meV, there are five possible transitions, labeled (i)–(v) in Fig. 8(a). It is these transitions that are responsible for the five spectral peaks of the dotted line of the spectrum of Fig. 4(b). The spectral peaks are actually slightly dispersive in nature implying the transitions are mixtures of absorption (solid arrows) and gain (dotted arrows). Note that the strength of the peaks depends on the competition between absorption and gain routes of equal energy. In Fig. 4(a) the absorption contribution to the spectral peak (iii) at $\hbar\omega = 125$ meV is almost zero due to an equal number of three absorption and gain routes. Compare this with the relatively stronger absorption contribution to the spectral peak (i) at $\hbar\omega \sim 110$ meV due to one absorption route but no corresponding gain route of this energy.

A rather different picture emerges when the second harmonic beam is switched on, i.e., all Rabi frequencies are $\Omega_1 = \Omega_2 = \Omega_3 = 5$ meV. Now the dressed state eigenvectors are

$$|a\rangle = \frac{1}{\sqrt{2}}(|3\rangle - |1\rangle), \quad |b\rangle = \frac{1}{\sqrt{2}}(|2\rangle - |1\rangle),$$

$$|c\rangle = \frac{1}{\sqrt{3}}(|1\rangle + |2\rangle + |3\rangle). \tag{11}$$

Importantly, eigenvectors $|a\rangle$ and $|b\rangle$ are degenerate in energy reducing the sets of triplets [described by Eq. (10)] to doublets. These doublets are closely analogous to the dressed states as expected for a bare state two-level system driven by a single coupling field. The number of spectral peaks is reduced from five to three as observed in Fig. 8(b) as only three transitions can now occur.

IV. CONCLUSIONS

In conclusion we have studied the effect of applying resonant coupling fields to all possible transitions in an asymmetric quantum well. The quantum well absorption recovers from a saturated spectrum when the Rabi frequencies of all three coupling fields are the same. The recovery of the absorption was described as arising from optically mediated coherent population trapping in the lowest level. The systems' spectral characteristics were also investigated and it was found that the system reduces from a (bare state) three-level quantum well to an effective two-level bare state quantum well as revealed by a dressed state analysis. Such systems might find applications in solid state optical switching schemes.

ACKNOWLEDGMENT

Financial support from the UK Engineering Physical Research Council is gratefully acknowledged.

*Electronic address: j.dynes@imperial.ac.uk

[1] D. E. Nikonov, A. Imamoglu, L. V. Butov, and H. Schmidt, Phys. Rev. Lett. **79**, 4633 (1997).

[2] D. E. Nikonov, A. Imamoglu, and M. O. Scully, Phys. Rev. B **59**, 12 212 (1999).

[3] P. M. Alsing, D. H. Huang, D. A. Cardimona, and T. Apostolova, Phys. Rev. A **68**, 033804 (2003).

[4] J. F. Dynes, M. D. Frogley, M. Beck, J. F. Faist, and C. C. Phillips, Phys. Rev. Lett. **94**, 157403 (2005).

[5] G. B. Serapiglia, E. Paspalakis, C. Sirtori, K. L. Vodopyanov, and C. C. Phillips, Phys. Rev. Lett. **84**, 1019 (2000).

[6] M. C. Phillips, H. Wang, I. Rumyantsev, N. H. Kwong, R. Takayama, and R. Binder, Phys. Rev. Lett. **91**, 183602 (2003).

[7] S. M. Sadeghi, S. R. Leffler, and J. Meyer, Opt. Commun. **151**, 173 (1998).

[8] L. Silvestri, F. Bassani, G. Czajkowski, and B. Davoudi, Eur. Phys. J. B **27**, 89 (2002).

[9] S. M. Sadeghi, S. R. Leffler, and J. Meyer, Phys. Rev. B **59**, 15388 (1999).

[10] J. P. Marangos, J. Mod. Opt. **45**, 471 (1998).

[11] S. M. Goodnick and P. Lugli, *Hot Carriers in Semiconductors Nanostructures*, edite by J. Shah, Chap. 3, 219 (1992).

[12] A. V. Kuznetsov, Phys. Rev. B **44**, 8721 (1991).

[13] L. M. Narducci, M. O. Scully, G. L. Oppo, P. Ru, and J. R. Tredicce, Phys. Rev. A **42**, 1630 (1990).

[14] K. L. Vodopyanov, V. Chazapis, C. C. Phillips, B. Sung, and J. S.

Harris, Jr., Semicond. Sci. Technol. **12**, 708(1997).
[15] E. Kreyszig, *Advanced Engineering Mathematics* (Wiley, New York, 1988).
[16] A. S. Manka, E. J. D'Angelo, L. M. Narducci, and M. O. Scully, Phys. Rev. A **47**, 4236 (1993).
[17] B. R. Mollow, Phys. Rev. A **5**, 2217 (1972).
[18] M. Lax, Phys. Rev. **172**, 350 (1968).
[19] S. M. Sadeghi, S. R. Leffler, and J. Meyer, Phys. Rev. B **59**, 15388 (1999).